International Journal of Low-Carbon Technologies, 2024, **19**, 2093–2107
https://doi.org/10.1093/ijlct/ctae160
Original Article

Utilizing the thermal energy from natural gas engines and the cold energy of liquid natural gas to satisfy the heat, power, and cooling demands of carbon capture and storage in maritime decarbonization: engineering, enhancement, and 4E analysis

Tao Hai[1,2,3], Ali Basem[4,*], Hayder Oleiwi Shami[5], Laith S. Sabri[6], Husam Rajab[7], Rand Otbah Farqad[8], Abbas Hameed Abdul Hussein[9], Wesam Abed AL Hassan Alhaidry[10], Ameer Hassan Idan[11], Narinderjit Singh Sawaran Singh[3]

[1]School of Information and Artificial Intelligence, Nanchang Institute of science & Technology, 330108, Nanchang, China
[2]School of Computer and Information, Qiannan Normal University for Nationalities, Duyun, Guizhou, 558000, China
[3]Faculty of Data Science and Information Technology, INTI International University, 71800, Malaysia
[4]Faculty of Engineering, Warith Al-Anbiyaa University, Karbala 56001, Iraq
[5]Department of Accounting, Al-Amarah University College, Maysan, Iraq
[6]Department of Chemical Engineering, University of Technology- Iraq, Baghdad, Iraq
[7]College of Engineering, Mechanical Engineering Department, Alasala University, King Fahad Bin Abdulaziz Rd., P.O. Box: 12666, Amanah, 31483, Dammam, Kingdom of Saudi Arabia
[8]College of Dentistry, Alnoor University, Mosul, Iraq
[9]Ahl Al Bayt University, Karbala, Iraq
[10]College of Technical Engineering, National University of Science and Technology, Dhi Qar, 64001, Iraq
[11]Al-Zahrawi University College, Karbala, Iraq

*Corresponding author. Faculty of Engineering, Warith Al-Anbiyaa University, Karbala 56001, Iraq. E-mail: ali.basem@uowa.edu.iq

Abstract

The MEPC 80 session has revised the International Maritime Organization (IMO) greenhouse gas strategy, setting more ambitious decarbonization goals. Carbon capture and storage (CCS) technologies have shown promise in reducing maritime carbon emissions, although their high-energy requirements have often been neglected in previous research. This study introduces a novel system integrating a natural gas engine, CCS, an Organic Rankine Cycle (ORC), and a power turbine (PT). An exhaust gas bypass strategy is used to enhance engine performance at low and medium loads, channeling exhaust to the PT for power generation. The engine's waste heat is fully utilized for CCS via cold, heat, and power. The study compares various absorbents in the CCS system, including monoethanolamine and piperazine solutions, which show different carbon capture efficiencies. Additionally, CO_2 storage conditions are analyzed and compared. The proposed system shows potential for significantly reducing the Energy Efficiency Design Index for general cargo ships. The study addresses the high-energy demands of CCS by utilizing the engine's waste heat, transforming a potential drawback into a beneficial resource. By integrating the ORC and PT, the system not only captures carbon but also improves overall energy efficiency, presenting a promising solution for maritime decarbonization. The analysis of CO_2 storage conditions further enhances the understanding of effective carbon management. This innovative system demonstrates that with strategic integration and optimization, significant progress can be made toward achieving the stricter decarbonization targets set by the IMO while also enhancing the energy efficiency of maritime operations.

Keywords: greenhouse gas reduction; recovery of waste heat; marine engine; 4E analyses; Energy Efficiency Design Index

1 Introduction

According to the International Maritime Organization (IMO) [1], maritime transport, which facilitates almost 89% of global trade [2], is responsible for 2.88% of the total carbon dioxide output worldwide. As a result, the International Marine Organization has implemented several strategies to decrease emissions in the marine sector. These include the implementation of the Energy Efficacy Development Index (EEDI), the Energy Efficacy Existing Ship Indicator (EEXI), and the Carbon Intensity Index [3]. More precisely, the implementation of the EEXI began on 1 January 2023, as stated by Qu and colleagues [4]. Additionally, Stage III of the EEDI has been launched, as mentioned by Gutierrez-Romero and colleagues [5]. Moreover, the MEPC 80 session sets more ambitious objectives, including two major targets [6]: a minimum reduction of 20%, with a goal of 30%, in overall yearly greenhouse gas (GHG) emissions from global shipping by 2030, compared to the levels in 2008, and a minimum reduction of 70%, with a goal of 80%, by 2040, also relative to 2008 [7].

Received 17 May 2024; revised 12 July 2024; accepted 7 August 2024

Today, the use of renewable energy has become popular in most industrial processes and sectors such as building, agriculture, transportation, etc. [8, 9]. Biomass, solar, geothermal, and wind energies are among the most well known of these energy sources [10, 11]. The maritime sector is making significant strides toward eliminating carbon emissions entirely [12, 13]. Various methods to reduce carbon emissions have been suggested, including the use of substitute energy sources [14, 15], as well as the utilization of sustainable and eco-friendly energy sources, for instance, solar energy [16, 17] and wind energy [18], and the implementation of electrochemical storage systems [19]. Among these options, substitute energy sources have the greatest potential for immediate usage in marine environment applications due to their cost-effectiveness and feasibility [20, 21]. It is expected that natural gas will have a significant impact on the upcoming phase of the carbon-neutral plan due to its cost-effectiveness and widespread accessibility [22]. Nevertheless, it is important to acknowledge that while ammonia engines do not release CO_2, they can nevertheless have a substantial influence on the greenhouse effect as a result of N_2O and unburned NH_3 emissions [23]. Maritime natural gas engines, being more advanced, are projected to become the dominant force in the low-carbon technology market in the upcoming years [24].

Although gas-powered engines represent progress in reducing carbon emissions, they still generate carbon dioxide, which poses a challenge to achieving near-zero emissions. In order to reduce the carbon footprint of maritime vessels, it is essential to utilize technologies such as CCS and waste heat recovery (WHR) [25, 26]. These technologies have been identified as significant in mitigating the environmental impact, as supported by studies conducted by Jiang and colleagues [27], Park and colleagues [28], Zheng and colleagues [29], Baldasso and colleagues [30], Hoang [31], and Liu and colleagues [18]. In a recent study, Chu *et al.* [32] emphasized the crucial significance of sophisticated CCS technology in attaining near-zero emissions. They argued that relying just on renewable energy is insufficient to achieve net-zero emissions. Although the present expenses associated with CCS technology expenditures are substantial, they are anticipated to yield significant economic advantages in the long run. Three primary technological methods for CCS in maritime environments include postcombustion, precombustion, and oxyfuel technologies [33]. In their study, Yao and colleagues [34] described a sophisticated oxy-combustion CCS system that is specifically tailored for marine engines. This system effectively utilizes waste heat from CCS to facilitate the evaporation of liquid natural gas (LNG). Their research revealed that the system could attain a carbon capture purity of 97.09%, an exergy efficiency of 51.78%, an output power of 318.36 kW, and an annual net profit of US$485165. Furthermore, postcombustion CCS is especially well suited for maritime natural gas engines because of the straightforward integration of the engine with the CCS system. Postcombustion processes generally exhibit higher carbon capture efficiency relative to precombustion and oxyfuel methods [35].

Feenstra and colleagues [36] investigated the application of a CCS system on LNG-powered ships. They discovered that the lowest possible expense for capturing and converting carbon dioxide into liquid form might be as little as 98 € per metric ton of CO_2. Zhou *et al.* evaluated the efficacy of CCS systems with varying CO_2 storage capacities, demonstrating that greater storage capacity resulted in reduced costs for liquefaction. Ros *et al.* [37] performed an economic evaluation of solvent-based CO_2 capture for marine uses, demonstrating that onboard CCS systems have the ability to capture CO_2 at a price of 118 €/ton CO_2, achieving an efficiency rate of 72.6%. Long and colleagues [38] developed a CCS system specifically designed for marine diesel engines. The system achieved an impressive carbon removal efficiency of 94.7%, which is equivalent to 1349 kg/h. Liu *et al.* [39] developed a controllable and rapid combustion concept for high power-density diesel engines. Stec and colleagues [40] devised a postcombustion CCS system specifically designed for maritime applications, which also effectively eliminates sulfur dioxide (SO_2). They emphasized that these systems have the ability to decrease CO_2 emissions with minimal decrease in energy efficiency in extremely cold temperatures. They can achieve carbon recovery rates ranging from 31.4% to 56.5% while still fulfilling the EEDI for the reference ship by 2025. Several research has concentrated on implementing CCS systems in maritime settings. Postcombustion procedures encompass techniques such as physical adsorption [41], chemical absorption [42], and membrane technology [43].

Chemical absorption has demonstrated significant potential because of its reliable performance and capacity to manage large amounts of gas [44–47]. In their study, Oh and colleagues [48] examined the effects of different sizes of monoethanolamine (MEA)-based aboard carbon containment systems regarding exhaust gas parameters. They determined system scale had little influence on the reduction of CO_2, indicating that smaller systems could potentially lead to cost savings. In their study, Manimaran *et al.* [49] investigated the utilization of phase change solvents to capture carbon from diesel engine exhaust. Specifically, they examined the effectiveness of two amino acids, L-alanine and L-arginine. These findings indicate that L-alanine led to a reduction in CO_2 emissions by 13.04%, while L-arginine achieved a reduction of 21.73%. In their study, Luo and Wang [50] devised a solvent-based CCS system specifically designed for cargo ships. This system successfully achieved a remarkable 73% decrease in carbon emissions from two 4-stroke engines, which collectively generated 17 MW of power. The cost of implementing this system amounted to 77.5 €/ton of CO_2. In addition, they implemented an improved system that includes an additional power turbine (PT), resulting in a carbon recovery rate of 90%, albeit at a higher expense. Multiple solvents are appropriate for absorption-based CCS devices. Nevertheless, postcombustion CCS systems require substantial quantities of thermal energy and power. Zhao and colleagues [51] performed a thermodynamic assessment of the absorption-based carbon capture process, illustrating a technique for transferring thermal energy into electricity to enable chemical reactions. Kim *et al.* [52] devised and assessed a portable carbon capture device for commercial vehicles with the aim of reducing GHG emissions. García-Mariaca and colleagues [53] suggested using an Organic Rankine Cycle (ORC) as a means to reduce the energy expenses linked to mobile engine carbon capture, resulting in a capture rate of 90%. In addition, the ORC was able to decrease the energy penalty on the engine's power by a range of 3.9% to 13.9% as a result of the CCS technology. Voice and Hamad [54] developed a CCS system tailored for internal combustion engines. This system effectively utilizes the engine's waste heat to maintain steady operation of the CCS system. These studies suggest that postcombustion, chemical capture, and liquefied containment CCS systems are highly

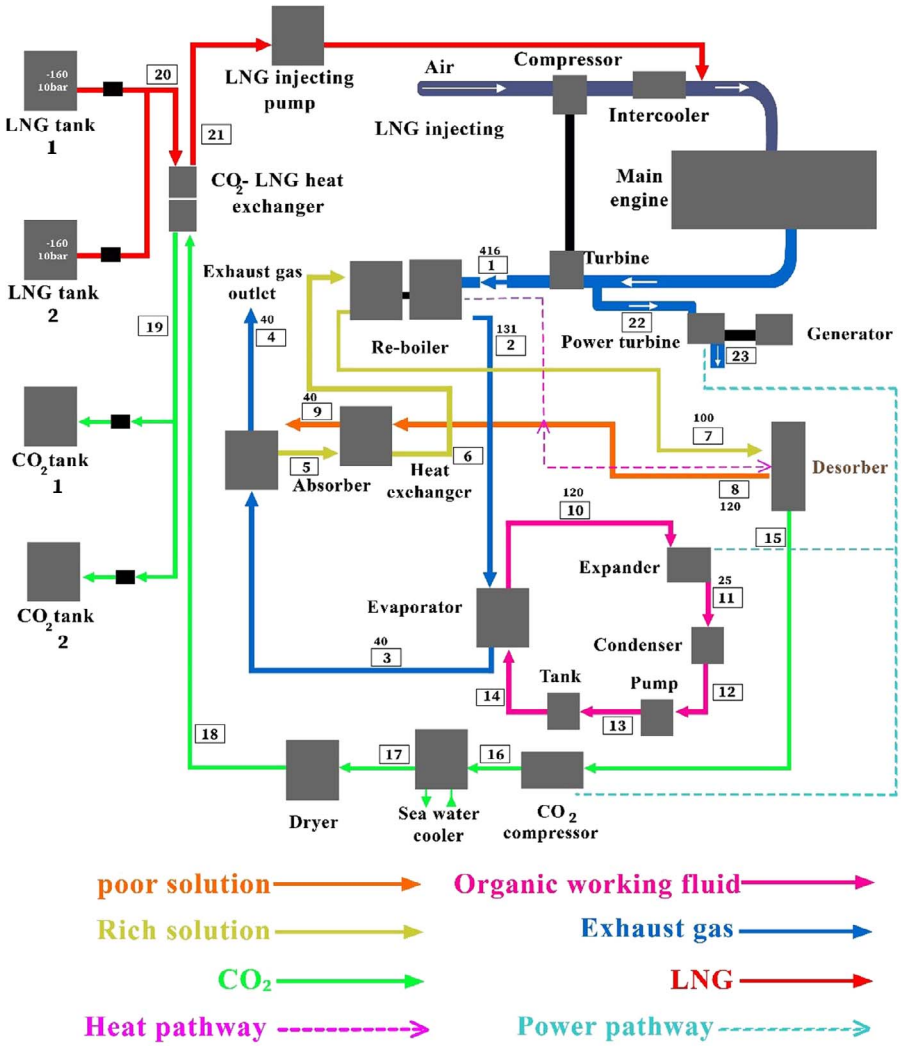

Figure 1. The illustration of the proposed energy system.

likely to be beneficial for maritime natural gas engines. Nevertheless, they also emphasize the significant need for heat, cold, and electricity necessary for CCS operations. Numerous researches have investigated the utilization of waste heat to fulfill the energy requirements of CCS systems. However, there is still a dearth of thorough and all-encompassing studies on the integration of engines, WHR systems [55], and CCS systems. Furthermore, in order to effectively absorb carbon dioxide in CCS systems, it is necessary to keep the temperature below 40°C. However, this need results in the inefficient use of low-temperature heat. No reports have been made regarding the utilization of waste heat at low temperatures. Moreover, earlier studies on postcombustion CCS systems have failed to consider the requirement of cold energy for compressing carbon dioxide. Ultimately, there is a dearth of comprehensive solutions for aligning CCS energy requirements with the provision of heat, cold, and power derived from waste heat from engines and cold energy from LNG. This article suggests the integration of maritime natural gas engines with CCS systems, along with the inclusion of WHR technology in both the engine and CCS system, as a solution to tackle these difficulties. Initially, it is recommended to redirect the exhaust gas away from the turbine under specific load levels, enabling the utilization of the residual thermal and pressure power by a PT. This method aids in optimizing the performance of the engine under varying load conditions. Furthermore, the excess thermal energy preceding the absorption tower in the CCS configuration is harnessed through the utilization of an ORC. Furthermore, the thermal energy generated during the carbon dioxide liquefaction process is used to convert LNG from liquid to gas and to heat it beforehand. Conversely, the cryogenic energy obtained from the LNG is utilized to liquefy carbon dioxide. A comparative assessment is carried out to evaluate the effectiveness of MEA and piperazine (PZ) as absorbent agents. Furthermore, a comparison investigation of two different CO_2 storage scenarios is also conducted. Moreover, the waste thermal energy generated by the engine's exhaust gas is utilized to aid in the process of desorption. An extensive analysis is performed to assess the effects of the suggested integration approach on energy efficiency, economic feasibility, and environmental advantages. This analysis covers four key aspects: energy, exergy, economic, and environmental. Parameter analysis is then conducted to determine the most favorable arrangement of the integrated system. Furthermore, a technical and economic evaluation of this integrated system is conducted. Ultimately, the environmental impacts of the integrated system are examined, specifically in relation to its implementation on a general cargo vessel. This study seeks

Table 1. Key specifications of the 8M23G natural gas engine

Parameter	Value	Parameter	Value
Numbers of cylinder	8	Rating power	1.6 MW
Bore	0.23 m	Compression ratio	13
Rating speed	1000 rpm	Average pressure	18.2 bar
Stroke	0.32 m		

to provide a robust approach for integrating maritime natural gas engines, CCS systems, and WHR systems.

2 System description

Fig. 1 illustrates the system being analyzed. This study focuses on a marine engine that runs on natural gas and operates at a medium speed. The precise details of the engine may be found in Table 1. At first, a fraction of the gas that is released from the cylinder (known as Stream 22) is redirected in order to maintain a consistent and reliable performance of the turbocharger. The PT captures the remaining thermal and pressure energies from the redirected gas. In addition, the exhaust gas that comes out of the turbocharger (Stream 1) is processed by chilling it using a concentrated solution (Stream 6). Extracting CO_2 from exhaust gas in a transmitter at a reduced temperature is of utmost importance. Consequently, the exhaust gas that has been cooled (Stream 2) experiences more cooling, resulting in the generation of some excess thermal energy. The waste thermal energy is subsequently harnessed by a straightforward ORC. Following a proper cool down process, the exhaust gas (Stream 3) is introduced into the absorber, resulting in the release of purified exhaust gas (Stream 4). Inside the transmitter, carbon dioxide (CO_2) from the exhaust gas interacts with either MEA or PZ solution, resulting in the formation of a solution enriched with CO_2 (Stream 5) that exits the absorber. The enriched solution is first heated by the cooler, CO_2-depleted solution (Stream 8), after that with the exhaust gas (Stream 1). Heated solution containing high levels of CO_2 (Stream 7) is subsequently introduced into the desorber, where the CO_2 is extracted from the solution and released. The solution with reduced CO_2 levels (Stream 8) is chilled by the incoming solution with higher CO_2 levels (Stream 5) in a heat exchanger specifically constructed for solutions with different CO_2 concentrations. This cooling process occurs before the solution re-enters the absorber to restart the cycle of absorbing CO_2. The CO_2 emitted from the desorber undergoes compression, cooling through seawater, dehydration, and ultimately complete liquefaction through LNG, before being stored in a CO_2 tank. The desorption process is fuelled by the heat generated by the exhaust gas.

3 Approaches

3.1 Engine evaluation

An engine evaluation was performed under atmospheric conditions with a temperature of 31.9°C and a humidity level of 54%. During this test, exhaust gas temperatures were measured upstream and downstream of the turbine, alongside the turbocharger speed, turbocharging pressure, and fuel usage.

3.2 Carbon capture system simulation

The study establishes a system-level carbon capture system model using Aspen Plus. The primary parts, the absorption and desorption units, are modeled using the RadFarc module, creating submodels based on rate analysis. The HeatX module simulates the thermal energy exchanger, and the heater module is employed for the condenser [56]. The chemical reactions between MEA and CO_2 are described below [57]:

$$2H_2O \rightleftarrows H_3O^+ + OH^- \tag{1}$$

$$HCO_3^- + H_2O \Longleftrightarrow CO_3^{2-} + H_3O^+ \tag{2}$$

$$HCO_3^- + H_2O \Longleftrightarrow CO_3^{2-} + H_3O^+ \tag{3}$$

$$CO_2 + OH^- \rightarrow HCO_3^{2-} \tag{4}$$

$$HCO_3^{2-} \rightarrow CO_2 + OH^- \tag{5}$$

$$MEA + CO_2 + H_2O \rightarrow MEACOO^- + H_3O^+ \tag{6}$$

$$MEACOO^- + H_3O^+ \rightarrow MEA + CO_2 + H_2O \tag{7}$$

The reaction rate constant of CO_2 absorption/desorption process has been simulated as given in the following equation:

$$r = kT^n \exp\left(-\frac{E}{RT}\right)\prod_{i=1}^{n} C_i^{a_i} \tag{8}$$

In the given formula, k is the pre-exponential coefficient, T indicates the temperature, E represents the activation energy, R stands as the universal gas constant, and C_i and a_i correspond the quantity and stoichiometric proportion of component i, respectively. The specifics of these responds are outlined in Table 2. Interactions between PZ and CO_2 are described below [58, 59]:

$$PZ + CO_2 \rightleftarrows H^+PZCOO^- \tag{9}$$

$$H^+PZCOO^- \rightleftarrows PZCOO^- + H^+ \tag{10}$$

$$PZCOO^- + CO_2 \Longleftrightarrow O^-OCPZCOO^- \tag{11}$$

$$PZ + H^+ \rightleftarrows PZH^+ \tag{12}$$

The carbon capture model was verified using data from Ref. [60] to validate the precision of the model described in this paper. The model was tested under two different operational conditions, resulting in comparative discrepancies of 3.17% and 2.29%. These discrepancies primarily originate from not accounting for heat losses in the heat exchangers. There were also slight discrepancies in flue gas temperature and pressure across the two datasets. However, the model established in this study meets the set error criteria and provides a reliable analysis of the carbon capture system operations. The efficiency of the carbon capture system is evaluated using the reboiler load per unit mass of CO_2, which is determined as follows:

$$q_{re} = \frac{Q_{re}}{m_{co_2}^{abs}} \tag{13}$$

Table 2. Variables of reaction period

Parameter	Reaction 4	Reaction 5	Reaction 6	Reaction 7
Activation energy	55.4 kJ/mol	123.1 kJ/mol	41.2 kJ/mol	65.5 kJ/mol
Pre-exponential factor	4.32E+13	2.38E+17	9.77E+10	3.23E+19

Table 3. Exergy loss formulations for each element of the proposed system

Component	Destructed exergy	Component	Destructed exergy
Turbine	$E10-E11-WT, ORC$	Intercoller 1	$Q1+E15a-E15b$
Condenser	$E11-Qc-E12$	Intercoller 2	$Q2+E15c-E16$
Pump	$E12-E13+WP, ORC$	Compressor—first step	$W1-E15-E15a$
Desorber	$E7-E15-E8$	Compressor—second step	$W2+E15b-E15c$
Liquefier	$E18+E20-E19-E21$	Evaporator	$E2+E14-E3-E10$
Absorber	$E3+E9-E5-E4$	#HE-Rich-poor	$E5+E8-E6-E9$

3.3 Simulation of ORC unit

A standard ORC is utilized at low-grade waste thermal energy reclamation, depicted in Fig. 1 (Stream 10-11-12-13-14-10). The evaluation of the ORC adheres to the principles of the first law of thermodynamics [61–63]. The thermal balance in the evaporator is characterized below:

$$W_{CO_2} = m_{co_2}\frac{k}{k-1}R_g T_{in}\left(1-\pi^{\frac{x-1}{x}}\right) \tag{14}$$

The net outlet energy of the ORC is determined below:

$$W_{net,ORC} = W_{E,ORC} - W_{P,ORC} \tag{15}$$

The heat released by the condenser in the organic working fluid is calculated as follows:

$$Q_c = m_w\left(h_{12}-h_{11}\right) \tag{16}$$

The efficiency of the system is subsequently calculated as follows:

$$\eta_e = \frac{W_{net,ORC}}{Q_h} \tag{17}$$

3.4 Exergy evaluation

This paper carries out an exergy analysis of the combined system. The techniques for examining exergy losses are outlined in Table 3. The reference environmental conditions are set at 26°C and under a pressure of 1 bar. Within this framework, WCO_2-1 signifies the power output of the first CO_2 compressor, WCO_2-2 represents the energy output of the second CO_2 compressor, Qq1 is the chilling thermal energy of intercooler 1, Qq2 denotes the chilling thermal energy of intercooler 2, and Ei expresses the exergy at stream *i*, computed below:

$$E_i = m_i\left(h_i - h_{i,0} - T_0\left(s_i - s_{i,0}\right)\right) \tag{18}$$

In this case, h_i and s_i denote the enthalpy and entropy at stream, respectively. Conversely, $h_{i,0}$ and $s_{i,0}$ indicate the enthalpy and entropy of the constituent at stream i under standard environmental conditions. T_0 represents the ambient temperature.

3.5 Technical–economic analysis

This study performs a techno-economic analysis. The methodology for calculating the capital expenditure (CAPEX) is explained below [36]:

$$CAPEX = \frac{FCI}{0.8}\times\frac{i(i+1)^n}{(i+1)^n-1}, (FCI = TDPC+TIPC) \tag{19}$$

Table 3 details the methods used for analyzing exergy loss. The reference conditions, or dead state, are set at 26°C and under a pressure of 1 bar. In this context, WCO_2-1 and WCO_2-2 are the power outputs of the first and second CO_2 compressors, respectively. Qq1 and Qq2 are the cooling heat from intercooler 1 and intercooler 2, respectively. Ei is the exergy at stream i, computed as follows:

This document undertakes a techno-economic evaluation. The capital expenditure (CAPEX) is calculated using the approach described below [36]:

$$CAPEX_a = \frac{CAPEX}{n}, (OPEX = FOPEX + VOPEX) \tag{20}$$

Here, '*i*' represents the interest rate and '*n*' the service life. FCI stands for the fixed capital investment, TDPC denotes the total direct plant cost, TIPC represents the total indirect plant cost, and TEC stands for the total equipment cost. TEC can be estimated using Aspen Plus software. The annual capital expenditure is subsequently calculated as follows:

$$TDPC = 2.10\times TEC, (TIPC = 0.14\times TDPC) \tag{21}$$

Here, m_{fuel} represents the fuel consumption, W denotes the power input of the system, t refers to the operational time annually, and C_{fuel} is the cost of fuel. The costs associated with

Table 4. The findings related to engine exiting gas

Parameter	Load				
	50%	70%	90%	100%	110%
Mass flow rate of exhaust gas	4590.43 kg/h	6792.98 kg/h	8108.1 kg/h	9073.94 kg/h	10203.72kg/h
Exhaust gas temperature after turbocharger	436.8°C	441.5°C	424.4°C	411.8°C	411.5°C
Exhaust gas temperature before turbocharger	515.4°C	554.6°C	562.72°C	571.4°C	585.3°C
CO_2 mole fraction	3.62%	3.63%	3.62%	3.62%	3.61%
CO_2 mass flow rate	261.36 kg/h	386.1 kg/h	461.34 kg/h	515.8 kg/h	578.16 kg/h

capturing carbon dioxide are calculated as follows:

$$CCC = \frac{CAPEX_a + FOPEX_a + VOPEX_a}{m_{CO_{2-a}}} \tag{22}$$

where mCO_2-a indicates the annual amount of carbon dioxide captured.

3.6 EEDI calculation approach

Lee and colleagues [64] devised a method for determining the EEDI for ships equipped with CCS systems, detailed as follows:

$$EEDI = \frac{\left(\prod_n^{j=1} f_i\right)\left(\sum_{nME}^{i=1} P_{ME(i)} \times C_{PME(i)} \times SFC_{ME(i)} \times f_{co_2}\right) + (P_{AE} \times C_{FAE} \times SFC_{AE}) + PTI + EFF}{f \times V_{ref} \times Capacity} \tag{23}$$

In this framework, PME(i) denotes the power output of the main engine, CFME(i) indicates the carbon factor for natural gas, and SFCME(i) represents the specific fuel consumption of the main engine. PAE refers to the power output of the auxiliary marine generator set, CFAE is the carbon factor for the fuel used by the generator set, and SFCAE defines the specific fuel consumption of the marine generator set. V_{ref} is the vessel's design speed, capacity is the design deadweight, m_{capture} quantifies the carbon captured, and m_{exhaust} specifies the mass flow rate of carbon dioxide in the exhaust gases. Additionally, the desired EEDI can be computed below:

$$EEDI_{required} = (1 - X\%) \times a \times DWT^{-c} \tag{24}$$

Here, X represents the decrement factor, whereas a and c denote coefficients meanwhile DWT stands for the vessel's deadweight.

4 Findings

4.1 Results of engine testing

The Marine 8M23G gas-powered engines underwent testing within the specified boundary conditions for an integrated CCS-ORC-PT system. Table 4 demonstrates that the temperatures of the exhaust gas after the turbocharger were higher than 410°C, suggesting the existence of waste heat of excellent quality that is appropriate for generating electricity using the ORC. Prior to entering the turbocharger, temperatures above 520°C were measured, highlighting substantial opportunities for power generation through power turbine (PT).

4.2 Analysis of parameters

4.2.1 Carbon capture unit

Fig. 2 illustrates the impact of different mass concentrations of MEA and PZ absorbents on the system's performance. The mass flow rates of these solutions decreased from 6.66 and 6.12 to 4.35 and 4.46 kg/s, respectively, when the concentration was increased from 20% to 40%. The drop is related to the increased efficacy of the absorbents at greater concentrations, resulting in a reduction in the amount needed. However, greater amounts of MEA are linked to a heightened risk of corrosive harm. The boiling points of MEA and PZ solutions decreased from 121°C to 122°C and from 123°C to 120°C, respectively, as the levels increased. This discovery indicates that PZ solutions have a more consistent temperature response when the concentration is altered, unlike MEA solutions. Raising the temperature can lead to more intense chemical reactions, highlighting the need to control the concentration of absorbent mass to prevent the breakdown of MEA and PZ at high temperatures. Moreover, the energy requirement of the reboiler shows a fluctuating trend in response to changes in the mass concentration of the absorbent. This behavior is influenced by various factors such as the higher temperature required for reboiling and the lower rate at which the absorbents flow. These factors contribute to the observed pattern. Fig. 2 illustrates that the ideal reboiler load is attained when the absorbent mass concentration is 30%, which is considered the benchmark.

In addition, Fig. 3 investigates the influence of CO_2 content in the impoverished solution on the operation of the CCS system. The reversible nature of the process of absorbing and desorbing CO_2 results in the presence of residual CO_2 in the solution with low concentration. When the CO_2 content in the inadequate solution increases from 0.16 to 0.29, the mass flow rate of the absorbent increases from 2.48 to 4.77 kg/s, and from 2.82 to 4.38 kg/s, respectively. This increase is a result of a decrease in the concentration of MEA or PZ. Furthermore, a rise in CO_2 concentration leads to a drop in the reboiler load per unit of CO_2 for the PZ solution. However, for the MEA solution, it initially falls and subsequently increases. Elevated levels of carbon dioxide (CO_2) decrease the amount of water present, resulting in a drop in the amount of heat required for evaporation and, thus, a reduction in the amount of CO_2 needed to operate the reboiler.

Raising the desorption pressure from 0.9 to 1.9 bar improves the rate at which CO_2 is released, leading to a drop in the amount of cooling water required, a reduction in chilling thermal power, and a rise in temperature from around 100°C to 120°C. Modulating the desorbing pressure is essential for maintaining an optimal temperature range. Moreover, raising the pressure at which desorption occurs

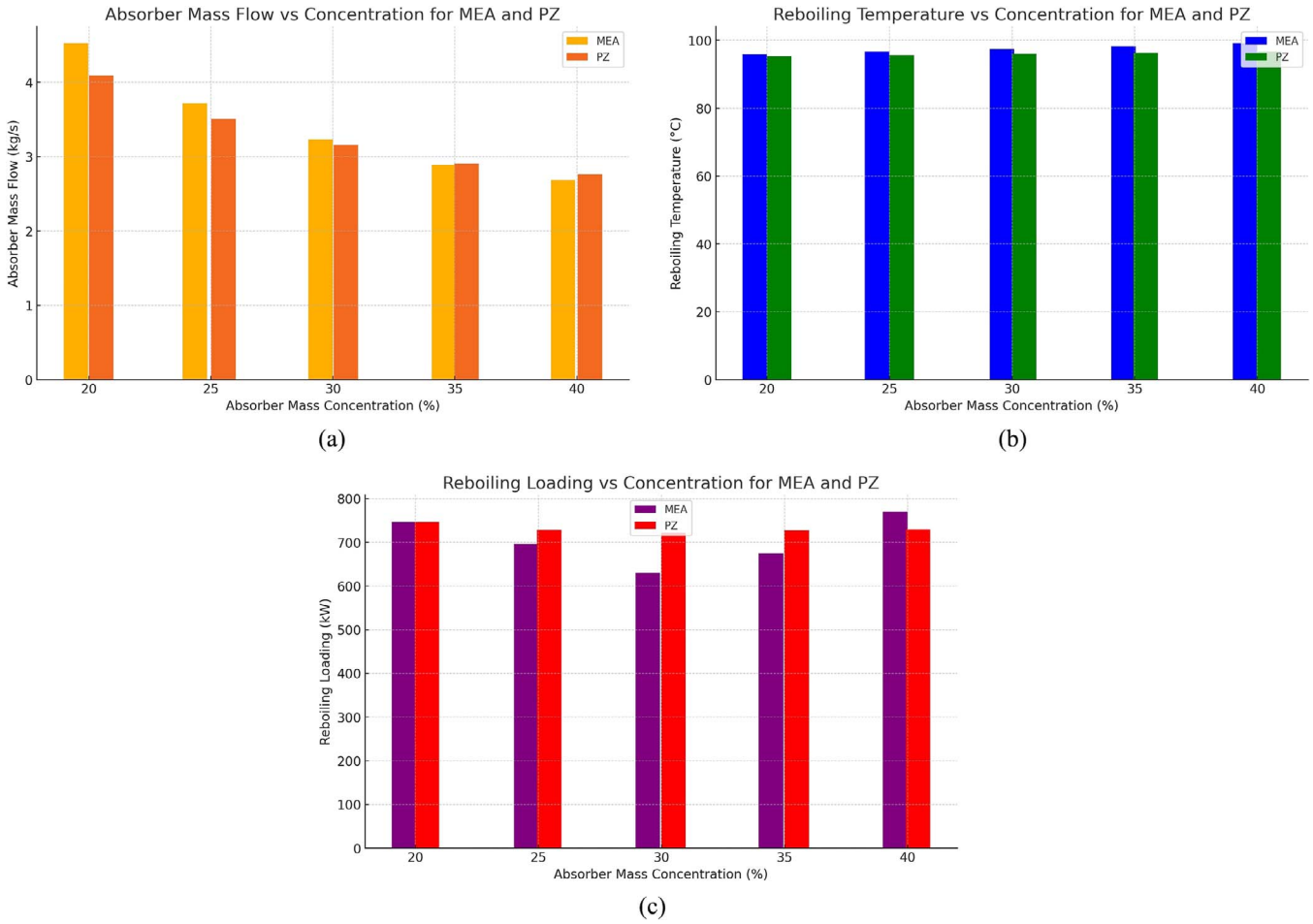

Figure 2. The impact of the absorption mass on (a) mass flow of the absorbent, (b) reboiler temperature, (c) loading of boiler.

reduces the amount of energy required per unit of CO_2 in the reboiler. Specifically, for the MEA solution, the energy load decreases from 2443 to 1688 kW/tCO_2, and for the PZ solution, it decreases from 2588 to 1916 kW/tCO_2. An increase in desorbing pressures causes a shift in the equilibrium toward producing more CO_2, reducing the amount of heat required for the desorption reaction. Nevertheless, higher desorbing pressures could elevate the energy demands for compressing and liquefying CO_2.

4.2.2 ORC unit

The primary parameters that significantly impact the efficiency of the ORC system are the pressures involved in the evaporation and condensation processes. The selection of organic working fluids is particularly critical, as they exhibit different evaporation temperatures at the same evaporating pressure. This study does a comprehensive examination of the evaporating and condensing temperatures in order to improve the heat integration between the exhaust gas and the ORC system. Fig. 4 illustrates the impact of the evaporation temperature on the performance of the ORC. An increase in the evaporation temperature often leads to a decrease in the required mass flow rate of the organic working fluid. However, the extent of this reduction varies depending on the specific fluids being used. Moreover, a higher evaporation temperature initially results in an elevation and, subsequently, a decline in power production, with distinct peak values for each fluid. These fluctuations are probably associated with the energy needs of the pump. Higher evaporating temperatures result in increased evaporating pressures, which can generate a substantial rise in the enthalpy change for the pump, exceeding the changes for the expander. Furthermore, increasing the temperature at which evaporation occurs continuously enhances thermal efficiency. As the temperature at which the liquid turns into vapor increases, the amount of heat required for the ORC decreases. Moreover, the power production and efficiency of the system are significantly influenced by the condensing temperature, as illustrated in Fig. 4. An increase in condensing temperature typically leads to decreased power output and efficiency. The decrease is attributed to the rise in the pump's power demand, which surpasses the power increase caused by the expander. Due to the constant thermal input in the ORC, the overall efficiency also drops.

4.3 Heat-electric-cold demand and supply matching

The PT is employed to absorb waste heat from diverted exhaust gases with high temperatures and pressures. Fig. 5 demonstrates that the power generation abilities of both the PT and the optimized ORC system vary under different operational situations. Significantly, when the engine's workload surpasses 50%, the outlet energy of the PT system varies from 8.86 to 69.12 kW for workloads ranging from 55% to 115%. Meanwhile, the net outlet energy of the ORC

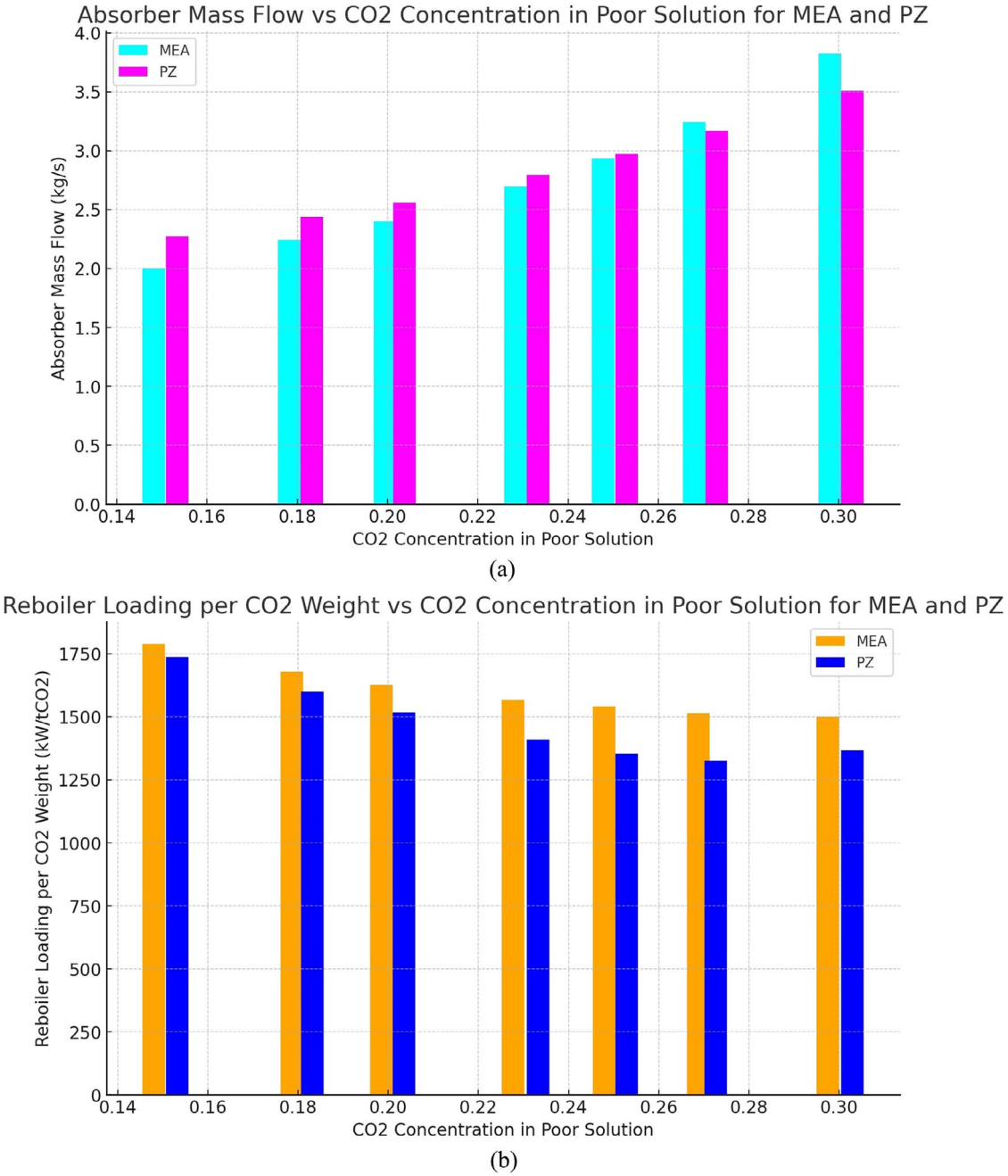

Figure 3. The impact of carbon dioxide in low solution on (a) absorbent mass flow and (b) the loading weight of reboiler.

system fluctuates between 15.05 and 33.46 kW when the engine loads increase from 50% to 110%. The main reason for these modifications is the higher temperatures of the exhaust gases both before and after the turbocharger, as well as the increased pressure of the exhaust gases before the turbocharger. These improvements greatly improve the energy outlet of the PT system relative to the ORC system. Moreover, the energy demands of the CCS system are effectively fulfilled by the collective power generated by both the PT and ORC systems. This integration not only enhances efficient energy consumption but also facilitates the necessary compression of CO_2 inside the CCS framework. Different quantities of electrical power are required for varying CO_2 storage pressures, as illustrated in Fig. 6. The electricity generated by the ORC and PT systems greatly exceeds the requirements for CO_2 compression in different storage situations, successfully supplying power for CO_2 compression activities. Additionally, the surplus electricity has the potential to replace some of the power generated by naval generators. Moreover, the process of converting CO_2 into a liquid state is made possible by utilizing the low-temperature energy obtained from LNG.

Fig. 7 illustrates the amount of cold energy required from LNG for CO_2 liquefaction, as well as the latent heat of LNG evaporation. The LNG cold energy effectively supports CO_2 liquefaction processes, regardless of storage circumstances.

4.4 Exergy evaluation findings

A comprehensive exergy study has been conducted on the proposed system, representing the distribution of exergy throughout the CCS system. The desorber experiences the highest level

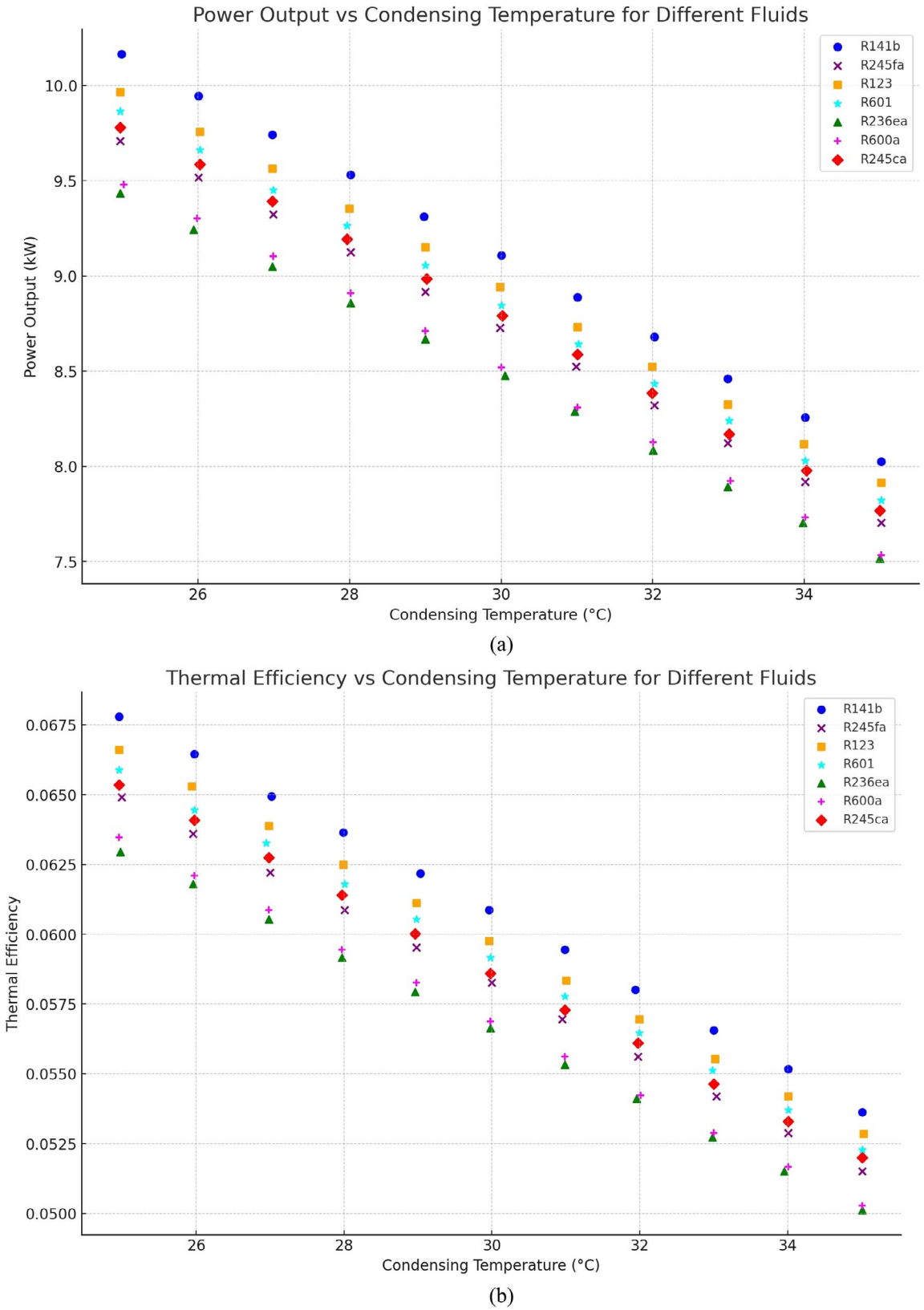

Figure 4. The impact of carbon dioxide in low solution on (a) absorbent mass flow and (b) the loading weight of reboiler.

of exergy destruction, mostly due to the combined effects of exergy losses from chemical reactions and high temperatures. The solution exergy has a notably high flow, indicating a substantial amount of chemical exergy. Following desorption, the exergy level of the solution significantly decreases compared to its initial state before absorption, primarily due to

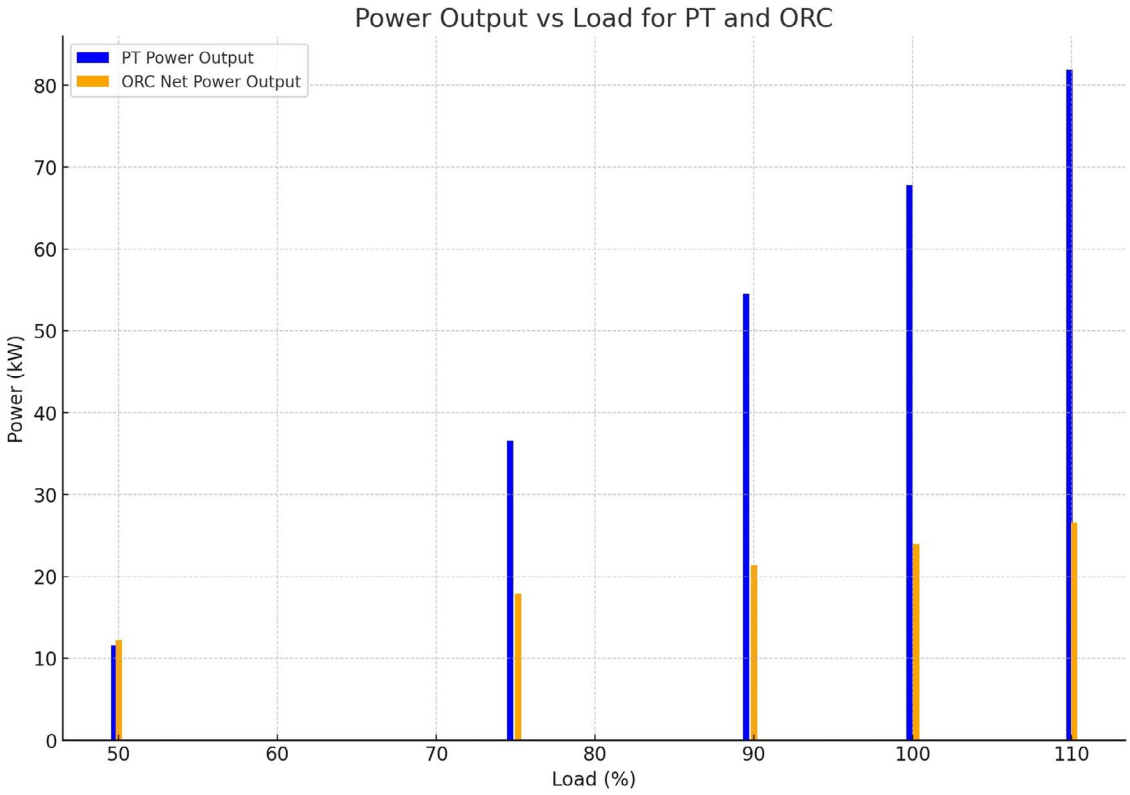

Figure 5. The impact of various loads on the power output.

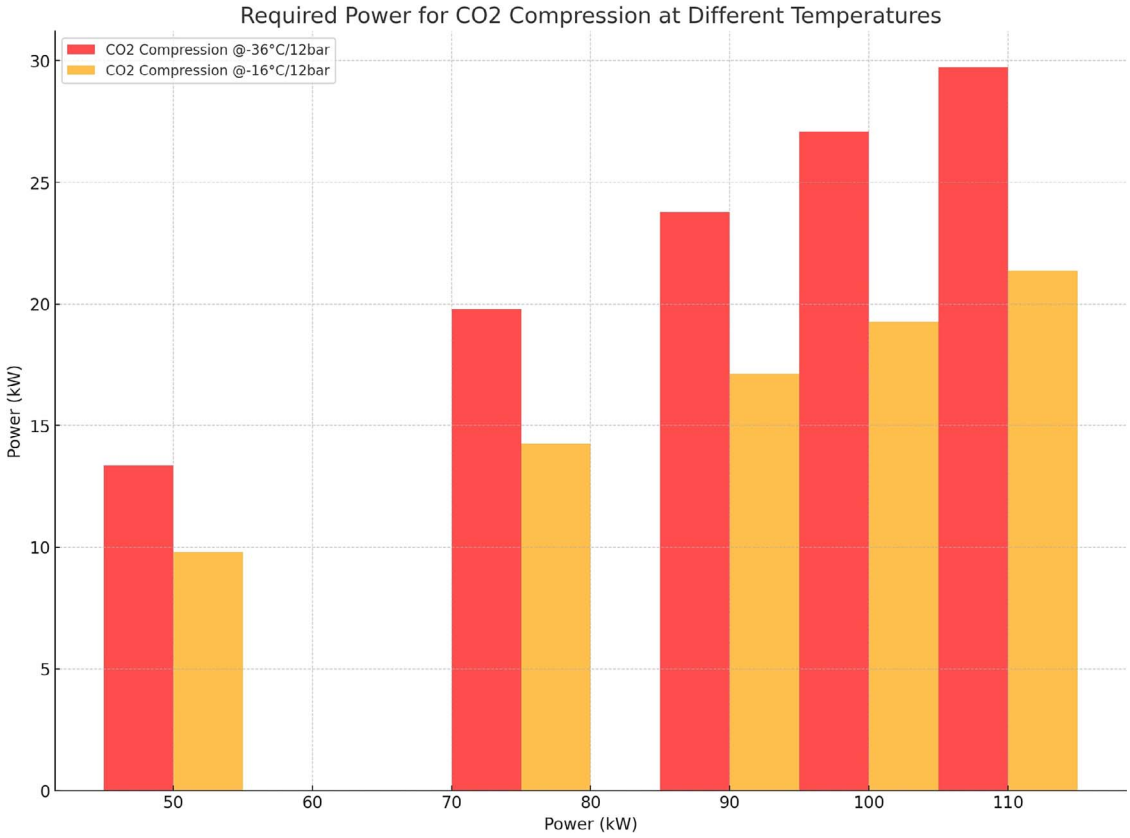

Figure 6. The outlet of power generation units in the proposed system and the required power for composing the CO_2 in various storage circumstances.

losses in the desorber and the requirement to replenish the solution before absorption. This is a major factor contributing to the significant exergy loss reported in the desorber. The CCS system achieves an exergy efficiency of 7.34%.

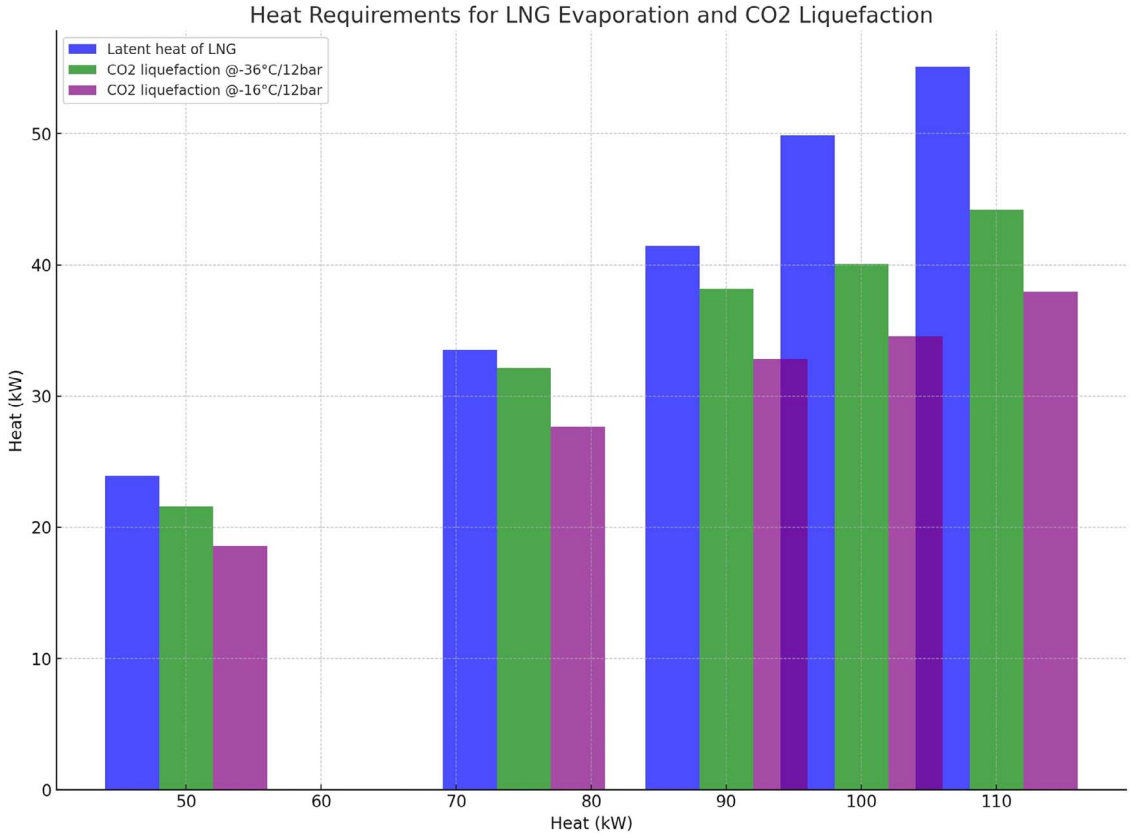

Figure 7. Comparing the needed cold energy for the liquefaction of carbon dioxide on different load conditions.

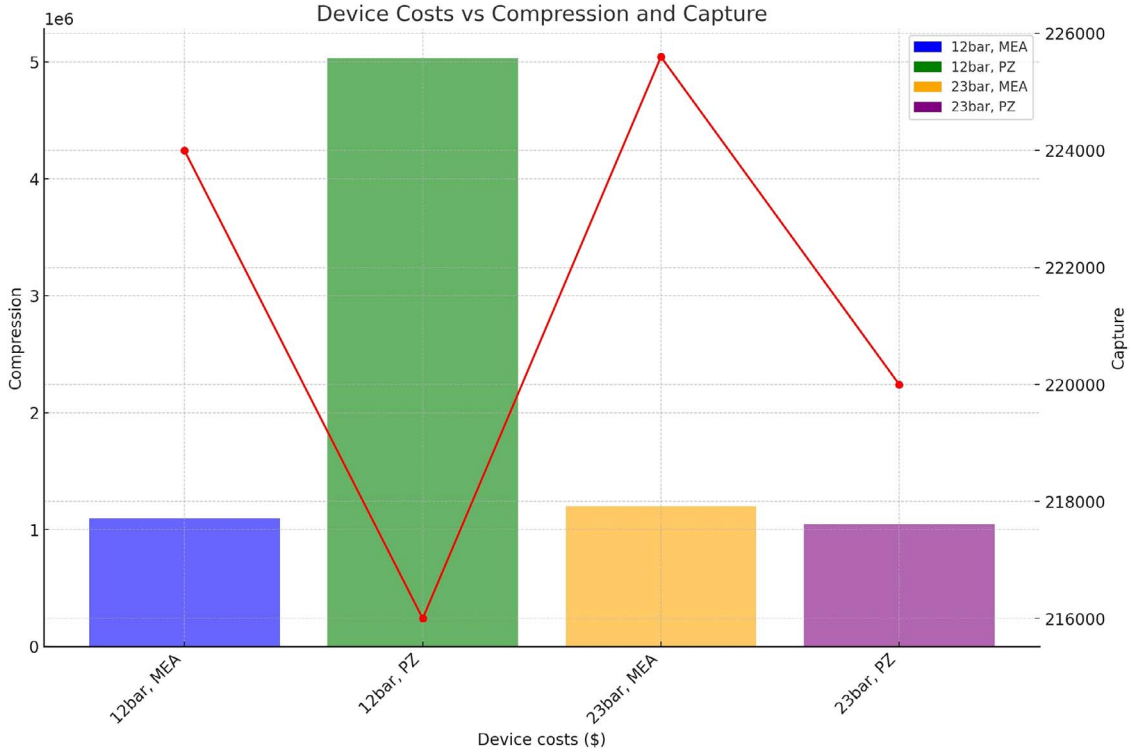

Figure 8. Device prices for the storage of the carbon dioxide unit.

4.5 Results of the techno-economic assessment

This research presents a detailed analysis of the integrated system, focusing on its technological and economic aspects. Fig. 8 illustrates the expenses related to the CCS system, considering various carbon dioxide storage pressures and types of solvents. The primary factors driving prices are compression

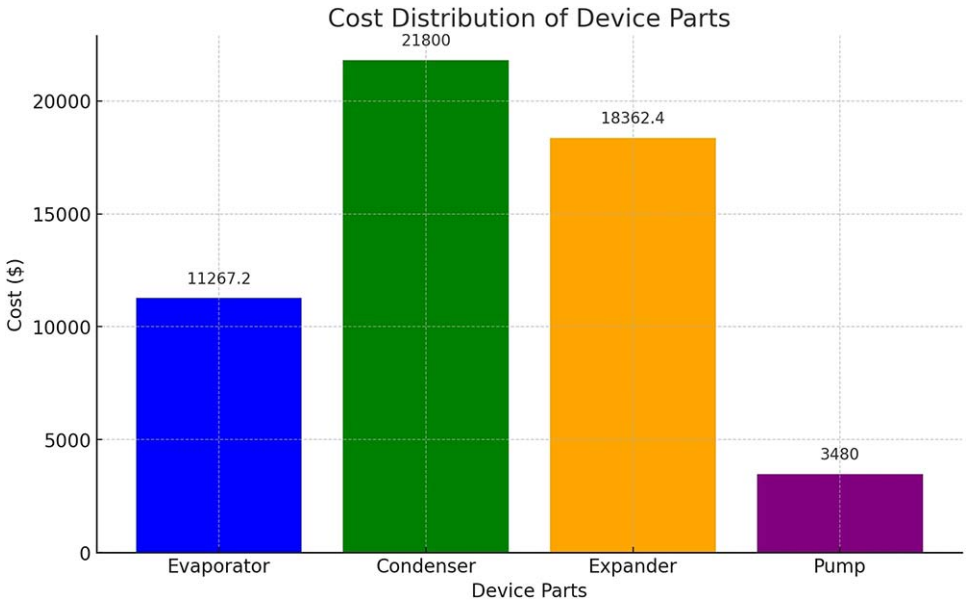

Figure 9. Device prices for the power generation cycle.

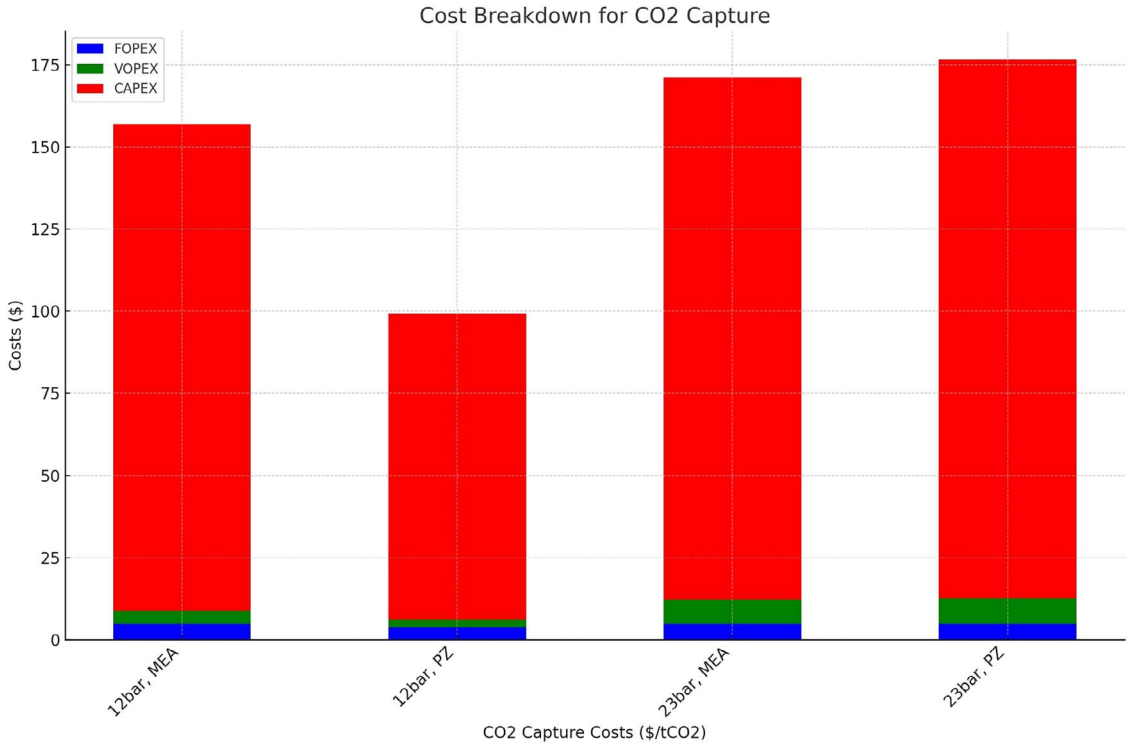

Figure 10. The carbon capture process's prices impacted by different conditions.

procedures, with costs being much greater at a storage pressure of 23 bars compared to 12 bars. In addition, the use of PZ as a solvent is more cost-effective compared to MEA. The most inexpensive choice is the 12-bar pressure situation with PZ. Fig. 9 illustrates the allocation of expenditures within the ORC system, with the condenser being the most expensive component and the pump incurring the lowest expenses. In general, the ORC system has considerably lower expenses compared to the CCS system. Fig. 10 provides further details on the expenses associated with carbon dioxide capture. It shows that the majority of the costs are attributed to capital expenditure (CAPEX), whereas operational expenditure (OPEX) and fixed operational expenditure (FOPEX) are significantly lower. The cost study for carbon dioxide capture indicates that the expenses per ton of CO_2 are \$196.20 for a 12-bar MEA configuration, \$124.03 for a 12-bar PZ configuration, \$214.01 for a 23-bar MEA configuration, and \$220.58 for a 23-bar PZ configuration. The cost variations result from the varying combinations of storage pressure and solvent choice.

5 Detailed roadmap for future work

Future work should focus on enhancing both the financial and energy efficiency of the CCS system to ensure its viability for widespread maritime application. Key areas for improvement include optimizing the integration of WHR and CCS technologies in a modular fashion to maximize energy savings and minimize costs. Advanced monitoring and control systems should be developed to reduce methane slip, which is crucial for achieving near-zero emissions in maritime operations. Additionally, further research is needed to explore alternative absorbents and their long-term effects on system performance and maintenance. Economic evaluations should consider a wider range of scenarios, including fluctuating fuel prices, varying carbon tax regimes, and different operational conditions, to provide a comprehensive understanding of the financial implications. Collaboration with industry stakeholders will be essential to address practical deployment challenges and to ensure that the proposed system meets regulatory requirements and operational constraints. By focusing on these areas, future studies can contribute significantly to advancing the effectiveness and adoption of CCS technologies in the maritime sector, thereby supporting global decarbonization efforts.

6 Summary and prospects

This paper presents a combined system that includes a CCS system, an (ORC) system, and an energy turret. The purpose of this system is to reach the demanding carbon footprint drop goals established by the updated IMO GHG strategy. The initial research involves conducting engine tests and analyzing the combined system parameters. The main objective is to compare the efficiency of PZ and MEA solvents in two different CO_2 storage circumstances. The system integration carefully synchronizes the engine outputs with the heat, cold, and electrical needs of the CCS system. When examined from thermodynamic, techno-economic, and environmental viewpoints, the system shows significant promise in decreasing maritime emissions. The key findings indicate that the performance of the CCS system is greatly affected by the concentration of the absorbent, the level of CO_2 in the depleted solution, and the pressure during desorption. The system's efficiency improves significantly as the concentration of CO_2 in the depleted solution increases and when higher desorption pressures is used. These factors substantially decrease the amount of heat needed for reboiling. The CCS system has determined the most efficient settings, which consist of a 30% concentration of absorbent, a depleted solution CO_2 concentration of 0.4 mol CO_2/mol PZ (or MEA), and a desorption pressure of 2 bar. The sequestration rate obtained using a PZ solution varies from 61.40% to 92.95% for engine loads ranging from 110% to 50%. On the other hand, MEA solutions produce capture rates between 84.81% and 97.64%.

The ORC PT technology effectively fulfills the power needs of the CCS system by utilizing waste heat from exhaust gases. The energy outputs exceed 99 and 109 kW, respectively, under particular conditions. Exergy evaluations identify the main causes of exergy loss in the CCS system, particularly due to solution losses, which lead to a low exergy efficacy of 7.35%. Nevertheless, the exergy efficacy of the carbon dioxide compression and liquefaction processes has the ability to achieve a maximum of 54.86%, but the ORC system has a strong exergy efficiency of 68.78%.

Cost evaluations indicate that the CCS system incurs significant charges, mostly due to compression costs. On the other hand, the ORC system experiences substantially reduced expenses. The cost of capturing carbon dioxide depends on the selection of solvent and storage pressure. It can range from \$196.20 per metric ton of CO_2 for a 12-bar MEA configuration to \$220.58 per metric ton of CO_2 for a 23-bar PZ configuration. This cutting-edge device provides a possible alternative for substantially mitigating carbon emissions from maritime vessels. The research employs a 7100-DWT general cargo ship to demonstrate that the suggested approach allows it to attain EEDI values that comfortably meet the Phase III criteria. The maximum decrease recorded in EEDI is 57.3%.

The present obstacles encompass the financial and energy effectiveness of the CCS system. Subsequent studies should prioritize enhancing these elements and more effectively incorporating WHR and CCS technologies modularly. Furthermore, it is crucial to tackle the issue of methane slip in order for CCS devices to successfully attain nearly zero emissions in maritime applications. Although it has some limits, this research sets the stage for a thorough comprehension and adoption of integrated technologies that could have a substantial impact on both market and policy frameworks in the maritime sector.

Acknowledgements

This work is supported by the science and technology foundation of Guizhou Province No. ZK(2024)661.

Author contributions

Tao Hai (Formal analysis [equal], Validation [equal], Writing—review & editing [equal]), Ali Basem (Methodology [equal], Project administration [equal], Writing—original draft [equal]), Hayder Shami (Resources [equal], Software [equal], Validation [equal]), Laith Sabri (Formal analysis [equal], Investigation [equal], Visualization [equal], Writing—review & editing [equal]), Husam Rajab (Data curation [equal], Formal analysis [equal], Validation [equal], Writing—review & editing [equal]), Rand Farqad (Formal analysis [equal], Investigation [equal], Writing—original draft [equal]), Abbas Abdul Hussein (Data curation [equal], Software [equal], Writing—review & editing [equal]), Wesam Abed Alhaidry (Data curation [equal], Validation [equal], Writing—review & editing [equal]), Ameer Idan (Conceptualization [equal], Funding acquisition [equal], Resources [equal], Writing—original draft [equal]), and Narinderjit Singh (Formal analysis [equal], Methodology [equal], Supervision [equal], Writing—review & editing [equal]).

Funding

None declared.

References

1. Joung T-H, Kang SG, Lee JK. *et al.* The IMO initial strategy for reducing Greenhouse Gas (GHG) emissions, and its follow-up actions towards 2050. *J Int Marit Saf Environ Aff Shipp* 2020;**4**: 1–7. https://doi.org/10.1080/25725084.2019.1707938.
2. Okumus D, Gunbeyaz SA, Kurt RE. *et al.* Towards a circular maritime industry: identifying strategy and technology solutions. *J Clean Prod* 2023;**382**:134935. https://doi.org/10.1016/j.jclepro.2022.134935.

3. IMO, T. *Guidelines on the Method of Calculation of the Attained Energy Efficiency Design Index (EEDI) for New Ships*. London, UK: International Maritime Organization, 2018.
4. Qu J, Feng Y, Zhu Y. *et al.* Assessment of a methanol-fueled integrated hybrid power system of solid oxide fuel cell and low-speed two-stroke engine for maritime application. *Appl Therm Eng* 2023;**230**:120735. https://doi.org/10.1016/j.applthermaleng.2023.120735.
5. Gutierrez-Romero JE, Esteve-Pérez J, Zamora B. Implementing Onshore Power Supply from renewable energy sources for requirements of ships at berth. *Appl Energy* 2019;**255**:113883. https://doi.org/10.1016/j.apenergy.2019.113883.
6. Feng Y, Chen J, Luo J. Life cycle cost analysis of power generation from underground coal gasification with carbon capture and storage (CCS) to measure the economic feasibility. *Resour Policy* 2024;**92**:104996. https://doi.org/10.1016/j.resourpol.2024.104996.
7. Technical Committee ISO/TC 207, I., 14040. *Environmental Management—Life Cycle Assessment—Principles and Framework* International Organization for Standardization, 2006;235–48.
8. Ghasemi A, Rad HN, Golizadeh F. A low-carbon polygeneration system based on a waste heat recovery system, a LNG cold energy process, and a CO2 liquefaction and separation unit. *Int J Low-Carbon Technol* 2024;**19**:654–66. https://doi.org/10.1093/ijlct/ctad146.
9. Rad HN, Ghasemi A, Akrami M. *et al.* Evaluating energy, exergy and economic aspects of a CO 2-free Kalina cycle cogeneration system with various solar collectors. *Int J Low-Carbon Technol* 2024;**19**:892–907. https://doi.org/10.1093/ijlct/ctae035.
10. Ghasemi A, Nikafshan Rad H, Akrami M. *et al.* Exergoeconomic and exergoenvironmental analyzes of a new biomass/solar-driven multigeneration energy system: an effort to maximum utilization of the waste heat of gasification process. *Therm Sci Eng Progr* 2024;**48**:102407. https://doi.org/10.1016/j.tsep.2024.102407.
11. Rad HN, Ghasemi A, Marefati M. Cost and environmental analysis and optimization of a new and green three-level waste heat recovery-based cogeneration cycle: a comparative study. *Heliyon* 2024;**10**:e29087. https://doi.org/10.1016/j.heliyon.2024.e29087.
12. Nejati MG, Kamali SE, Zoqi MJ. *et al.* Life cycle analysis (cost and environmental) of different renewable natural gas from waste procedures based on a multivariate decision-making approach: a comprehensive comparative analysis. *Int J Low-Carbon Technol* 2024;**19**:339–50. https://doi.org/10.1093/ijlct/ctae008.
13. Demir N, Shadjou AM, Abdulameer MK. *et al.* A low-carbon multigeneration system based on a solar collector unit, a bio waste gasification process and a water harvesting unit. *Int J Low-Carbon Technol* 2024;**19**:1204–14. https://doi.org/10.1093/ijlct/ctae045.
14. Dey S, Reang NM, das PK. *et al.* A comprehensive study on prospects of economy, environment, and efficiency of palm oil biodiesel as a renewable fuel. *J Clean Prod* 2021;**286**:124981. https://doi.org/10.1016/j.jclepro.2020.124981.
15. Liu L, Wu J, Liu H. *et al.* Investigation of combustion and emissions characteristics in a low-speed marine engine using ammonia under thermal and reactive atmospheres. *Int J Hydrogen Energy* 2024;**63**:1237–47. https://doi.org/10.1016/j.ijhydene.2024.02.308.
16. Zhu Y, Zhou S, Feng Y. *et al.* Influences of solar energy on the energy efficiency design index for new building ships. *Int J Hydrogen Energy* 2017;**42**:19389–94. https://doi.org/10.1016/j.ijhydene.2017.06.042.
17. Zhu C, Wang M, Guo M. *et al.* An innovative process design and multi-criteria study/optimization of a biomass digestion-supercritical carbon dioxide scenario toward boosting a geothermal-driven cogeneration system for power and heat. *Energy* 2024;**292**:130408. https://doi.org/10.1016/j.energy.2024.130408.
18. Liu F, Sun F, Wang X. Impact of turbine technology on wind energy potential and CO2 emission reduction under different wind resource conditions in China. *Appl Energy* 2023;**348**:121540. https://doi.org/10.1016/j.apenergy.2023.121540.
19. He G, Ciez R, Moutis P. *et al.* The economic end of life of electrochemical energy storage. *Appl Energy* 2020;**273**:115151. https://doi.org/10.1016/j.apenergy.2020.115151.
20. Bilgili L. A systematic review on the acceptance of alternative marine fuels. *Renew Sustain Energy Rev* 2023;**182**:113367. https://doi.org/10.1016/j.rser.2023.113367.
21. Zhu C, Zhang Y, Wang M. *et al.* Optimization, validation and analyses of a hybrid PV-battery-diesel power system using enhanced electromagnetic field optimization algorithm and ε-constraint. *Energy Rep* 2024;**11**:5335–49. https://doi.org/10.1016/j.egyr.2024.04.043.
22. Cao J, Dong D, Wei F. *et al.* Investigation on jet controlled diffusion combustion (JCDC) mode applied on a marine large-bore two-stroke engine. *J Clean Prod* 2023;**429**:139546. https://doi.org/10.1016/j.jclepro.2023.139546.
23. Sánchez A, Rengel MM, Martín M. A zero CO2 emissions large ship fuelled by an ammonia-hydrogen blend: reaching the decarbonisation goals. *Energ Conver Manage* 2023;**293**:117497. https://doi.org/10.1016/j.enconman.2023.117497.
24. Jang H, Jeong B, Zhou P. *et al.* Demystifying the lifecycle environmental benefits and harms of LNG as marine fuel. *Appl Energy* 2021;**292**:116869. https://doi.org/10.1016/j.apenergy.2021.116869.
25. Sun W, Zhang X, Liu B. *et al.* Analysis of the main influencing factors of waste heat utilization effectiveness in the tank storage receiving process of waxy crude oil under dynamic liquid level conditions. *Renew Energy* 2024;**228**:120707. https://doi.org/10.1016/j.renene.2024.120707.
26. Zhu C, Wang M, Guo M. *et al.* Optimizing solar-driven multigeneration systems: a cascade heat recovery approach for power, cooling, and freshwater production. *Appl Therm Eng* 2024;**240**:122214. https://doi.org/10.1016/j.applthermaleng.2023.122214.
27. Jiang Y, Mathias PM, Zheng RF. *et al.* Energy-effective and low-cost carbon capture from point-sources enabled by water-lean solvents. *J Clean Prod* 2023;**388**:135696. https://doi.org/10.1016/j.jclepro.2022.135696.
28. Park S, Mun H, Park J. *et al.* Cost optimization methodology based on carbon-techno-economic analysis: an application to post-combustion carbon capture process. *J Clean Prod* 2024;**434**:139887. https://doi.org/10.1016/j.jclepro.2023.139887.
29. Zheng C, Wu X, Chen X. Low-carbon transformation of ethylene production system through deployment of carbon capture, utilization, storage and renewable energy technologies. *J Clean Prod* 2023;**413**:137475. https://doi.org/10.1016/j.jclepro.2023.137475.
30. Baldasso E, Gilormini TJA, Mondejar ME. *et al.* Organic Rankine Cycle-based waste heat recovery system combined with thermal energy storage for emission-free power generation on ships during harbor stays. *J Clean Prod* 2020;**271**:122394. https://doi.org/10.1016/j.jclepro.2020.122394.
31. Hoang AT. Waste heat recovery from diesel engines based on Organic Rankine Cycle. *Appl Energy* 2018;**231**:138–66. https://doi.org/10.1016/j.apenergy.2018.09.022.
32. Chu B, Lin B, Tian L. *et al.* A long-term impact assessment of carbon capture (storage) investment conducted by conventional power company on sustainable development. *Appl Energy* 2024;**358**:122567. https://doi.org/10.1016/j.apenergy.2023.122567.
33. Davoodi S, al-Shargabi M, Wood DA. *et al.* Review of technological progress in carbon dioxide capture, storage, and utilization. *Gas Sci Eng* 2023;**117**:205070. https://doi.org/10.1016/j.jgsce.2023.205070.
34. Yao S, Li C, Wei Y. Design and optimization of a zero carbon emission system integrated with the utilization of marine engine waste heat and LNG cold energy for LNG-powered ships. *Appl Therm Eng* 2023;**231**:120976. https://doi.org/10.1016/j.applthermaleng.2023.120976.
35. Thaler B, Kanchiralla FM, Posch S. *et al.* Optimal design and operation of maritime energy systems based on renewable methanol and closed carbon cycles. *Energ Conver Manage* 2022;**269**:116064. https://doi.org/10.1016/j.enconman.2022.116064.

36. Feenstra M, Monteiro J, van den Akker JT. *et al.* Ship-based carbon capture onboard of diesel or LNG-fuelled ships. *Int J Greenh Gas Control* 2019;**85**:1–10. https://doi.org/10.1016/j.ijggc.2019.03.008.
37. Ros JA, Skylogianni E, Doedée V. *et al.* Advancements in ship-based carbon capture technology on board of LNG-fuelled ships. *Int J Greenh Gas Control* 2022;**114**:103575. https://doi.org/10.1016/j.ijggc.2021.103575.
38. Long NVD, Lee DY, Kwag C. *et al.* Improvement of marine carbon capture onboard diesel fueled ships. *Chem Eng Process-Process Intensif* 2021;**168**:108535. https://doi.org/10.1016/j.cep.2021.108535.
39. Liu L, Peng Y, Zhang W. *et al.* Concept of rapid and controllable combustion for high power-density diesel engines. *Energ Conver Manage* 2023;**276**:116529. https://doi.org/10.1016/j.enconman.2022.116529.
40. Stec M, Tatarczuk A, Iluk T. *et al.* Reducing the energy efficiency design index for ships through a post-combustion carbon capture process. *Int J Greenh Gas Control* 2021;**108**:103333. https://doi.org/10.1016/j.ijggc.2021.103333.
41. Ben-Mansour R, Habib MA, Bamidele OE. *et al.* Carbon capture by physical adsorption: materials, experimental investigations and numerical modeling and simulations–a review. *Appl Energy* 2016;**161**:225–55. https://doi.org/10.1016/j.apenergy.2015.10.011.
42. Salih HA, Pokhrel J, Reinalda D. *et al.* Hybrid–Slurry/Nanofluid systems as alternative to conventional chemical absorption for carbon dioxide capture: a review. *Int J Greenh Gas Control* 2021;**110**:103415. https://doi.org/10.1016/j.ijggc.2021.103415.
43. Chakrabortty S, Kumar R, Nayak J. *et al.* Green synthesis of MeOH derivatives through in situ catalytic transformations of captured CO2 in a membrane integrated photo-microreactor system: a state-of-art review for carbon capture and utilization. *Renew Sustain Energy Rev* 2023;**182**:113417. https://doi.org/10.1016/j.rser.2023.113417.
44. Ding S, Liu Y. Adsorption of CO2 from flue gas by novel seaweed-based KOH-activated porous biochars. *Fuel* 2020;**260**:116382. https://doi.org/10.1016/j.fuel.2019.116382.
45. Leung DY, Caramanna G, Maroto-Valer MM. An overview of current status of carbon dioxide capture and storage technologies. *Renew Sustain Energy Rev* 2014;**39**:426–43. https://doi.org/10.1016/j.rser.2014.07.093.
46. Mumford KA, Wu Y, Smith KH. *et al.* Review of solvent based carbon-dioxide capture technologies. *Front Chem Sci Eng* 2015;**9**:125–41. https://doi.org/10.1007/s11705-015-1514-6.
47. Wang M, Lawal A, Stephenson P. *et al.* Post-combustion CO2 capture with chemical absorption: a state-of-the-art review. *Chem Eng Res Des* 2011;**89**:1609–24. https://doi.org/10.1016/j.cherd.2010.11.005.
48. Oh J, Kim D, Roussanaly S. *et al.* Optimal capacity design of amine-based onboard CO2 capture systems under variable marine engine loads. *Chem Eng J* 2024;**483**:149136. https://doi.org/10.1016/j.cej.2024.149136.
49. Manimaran R, Mohanraj T, Prabakaran S. *et al.* Post combustion carbon capture from diesel engine exhaust using phase change solvents with absorption technique. *Mater Today Proc* 2022;**66**:1424–30. https://doi.org/10.1016/j.matpr.2022.05.300.
50. Luo X, Wang M. Study of solvent-based carbon capture for cargo ships through process modelling and simulation. *Appl Energy* 2017;**195**:402–13. https://doi.org/10.1016/j.apenergy.2017.03.027.
51. Zhao J, Fu J, Deng S. *et al.* Decoupled thermal-driven absorption-based CO2 capture into heat engine plus carbon pump: a new understanding with the case study. *Energy* 2020;**210**:118556. https://doi.org/10.1016/j.energy.2020.118556.
52. Kim J, Yoo Y, Kim S. *et al.* Design and assessment of a novel mobile carbon capture system: energy and exergy analyses. *Energ Conver Manage* 2024;**300**:117934. https://doi.org/10.1016/j.enconman.2023.117934.
53. García-Mariaca A, Llera-Sastresa E, Moreno F. Application of ORC to reduce the energy penalty of carbon capture in non-stationary ICE. *Energ Conver Manage* 2022;**268**:116029. https://doi.org/10.1016/j.enconman.2022.116029.
54. Voice AK, Hamad E. Evaluating the thermodynamic potential for carbon capture from internal combustion engines. *Transp Eng* 2022;**10**:100144. https://doi.org/10.1016/j.treng.2022.100144.
55. Basem A, Jasim DJ, Ghodratallah P. *et al.* Technical and financial feasibility of a chemicals recovery and energy and water production from a dairy wastewater treatment plant. *Sci Rep* 2024;**14**:11143. https://doi.org/10.1038/s41598-024-61699-8.
56. Zhu C, Zhang Y, Wang M. *et al.* Simulation and comprehensive study of a new trigeneration process combined with a gas turbine cycle, involving transcritical and supercritical CO2 power cycles and Goswami cycle. *J Therm Anal Calorim* 2024;**149**:6361–84. https://doi.org/10.1007/s10973-024-13182-9.
57. Mun J-H, Shin BJ, Kim SM. *et al.* Optimal MEA/DIPA/water blending ratio for minimizing regeneration energy in absorption-based carbon capture process: experimental CO2 solubility and thermodynamic modeling. *Chem Eng J* 2022;**444**:136523. https://doi.org/10.1016/j.cej.2022.136523.
58. Lim H, Kim K, Park HS. *et al.* Carbon dioxide capture in aqueous potassium serinate and piperazine solution using bubbling reactor for membrane contactor applications. *J Ind Eng Chem* 2023;**122**:200–9. https://doi.org/10.1016/j.jiec.2023.02.021.
59. Stowe HM, Paek E, Hwang GS. First-principles assessment of CO 2 capture mechanisms in aqueous piperazine solution. *Phys Chem Chem Phys* 2016;**18**:25296–307. https://doi.org/10.1039/C6CP03584A.
60. Dugas RE. Pilot plant study of carbon dioxide capture by aqueous monoethanolamine. Doctoral dissertation, University of Texas at Austin Libraries, 2006.
61. Ayadi B, Jasim DJ, Anqi AE. *et al.* Multi-criteria/comparative analysis and multi-objective optimization of a hybrid solar/-geothermal source system integrated with a carnot battery. *Case Stud Therm Eng* 2024;**54**:104031. https://doi.org/10.1016/j.csite.2024.104031.
62. Bai L, Asadollahzadeh M, Chauhan BS. *et al.* A new biomass-natural gas dual fuel hybrid cooling and power process integrated with waste heat recovery process: exergoenvironmental and exergoeconomic assessments. *Process Saf Environ Prot* 2023;**176**:867–88. https://doi.org/10.1016/j.psep.2023.06.037.
63. Marefati M, Mehrpooya M, Pourfayaz F. Performance analysis of an integrated pumped-hydro and compressed-air energy storage system and solar organic Rankine cycle. *J Energy Storage* 2021;**44**:103488. https://doi.org/10.1016/j.est.2021.103488.
64. Lee S, Yoo S, Park H. *et al.* Novel methodology for EEDI calculation considering onboard carbon capture and storage system. *Int J Greenh Gas Control* 2021;**105**:103241. https://doi.org/10.1016/j.ijggc.2020.103241.